Biosafety and Health 7 (2025) 152–165

Contents lists available at ScienceDirect

Biosafety and Health

journal homepage: www.elsevier.com/locate/bsheal

Original Research

Longitudinal profiling of host response and oropharyngeal respiratory microbiome reveals dynamic alterations during recovery from community-acquired pneumonia

Lizhe Hong [a,b,1], Lijun Suo [c,1], Kang Chang [b,1], Hongyun Cao [c], Jiahui Luan [c], Fuxin Zhang [c], Xiaofeng Yu [c], Xiaohui Zou [b,*], Bo Liu [c,d,*], Bin Cao [a,b,2,*], CAP-China Network

[a] Chinese Academy of Medical Sciences and Peking Union Medical College, Beijing 100730, China
[b] National Center for Respiratory Medicine, State Key Laboratory of Respiratory Health and Multimorbidity, National Clinical Research Center for Respiratory Diseases, Institute of Respiratory Medicine, Chinese Academy of Medical Sciences, Laboratory of Clinical Microbiology and Infectious Diseases, Department of Pulmonary and Critical Care Medicine, Center of Respiratory Medicine, China-Japan Friendship Hospital, Beijing 100029, China
[c] Department of Clinical Microbiology, Pulmonary and Critical Care Medicine, Zibo City Key Laboratory of Respiratory Infection and Clinical Microbiology, Zibo City Engineering Technology Research Center of Etiology Molecular Diagnosis, Zibo Municipal Hospital, Zibo 255013, China
[d] Department of Pulmonary and Critical Care Medicine, Shandong Institute of Respiratory Diseases, The First Affiliated Hospital of Shandong First Medical University, Shandong Provincial Qianfoshan Hospital, Shandong University, Jinan 250014, China

ARTICLE INFO

Article history:
Received 18 November 2024
Revised 14 May 2025
Accepted 14 May 2025
Available online 15 May 2025

Keywords:
Community-acquired pneumonia (CAP)
Transcriptome
Respiratory microbiome
Recovery

ABSTRACT

Community-acquired pneumonia (CAP) is a major global health concern, with limited understanding of longitudinal changes in host gene expression and respiratory microbiome throughout disease progression and recovery. To address this gap, we longitudinally collected CAP patients' peripheral blood for transcriptome and oropharyngeal swabs for microbiome analysis from admission to 4 months post infection. Age- and sex-matched volunteers were recruited as controls. We observed CAP patients mounted rapid, effective, and moderate immune responses against infection. Coagulation activation and mitochondrial dysfunction were the striking pathways showing distinct difference in CAP patients compared to controls, and the latter was validated by lower adenosine triphosphate (ATP) levels in the peripheral blood mononuclear cells (PBMCs) of CAP patients. Although transcriptional perturbations gradually decreased, they did not fully recover during the follow-up period. Similarly, persisting oropharyngeal microbiome dysbiosis was observed, characterized by significantly lower alpha diversity and altered taxonomy distribution ($P < 0.05$). CAP increased the relative abundance of *Streptococcus, Veillonella*, and *Peptostreptococcus*, while decreasing that of *Haemophilus*, *Neisseria*, and *Porphyromonas*. Integrated analysis of host response and oropharyngeal microbiome revealed that the relative abundance of *Haemophilus*, *Neisseria*, *Porphyromonas*, and *Stomatobaculum* were positively related to mitochondrial structure and function pathways, whereas the relative abundance of *Prevotella* declined over time in patients and positively correlated with anti-pathogen and interferon signaling pathways. These results underscore the persistent impact of CAP on both host immunity and oropharyngeal microbiome, even months after infection, emphasizing the need for long-term follow-up and targeted strategies to facilitate full recovery and restore homeostasis.

1. Introduction

Community-acquired pneumonia (CAP) continues to be one of the most common infectious diseases and the leading global burden, especially among the elderly [1–3]. According to the estimation of the World Health Organization (WHO), lower respiratory tract infection is the globally deadliest communicable disease, which claimed 2.6 million lives in 2019 [3]. The pandemic of coronavirus disease 2019 (COVID-19) during the past few years makes the CAP a high-priority problem concerned worldwide.

* Corresponding authors: Center of Respiratory Medicine, China-Japan Friendship Hospital, Beijing 100029, China (X. Zou and B. Cao); Department of Clinical Microbiology, Pulmonary and Critical Care Medicine, Zibo Municipal Hospital, Zibo 255013, China (B. Liu).
E-mail addresses: zouxiaohui17@163.com (X. Zou), 42820159@qq.com (B. Liu), caobin_ben@163.com (B. Cao).
[1] These authors contributed equally to this work.
[2] Given his role as Editorial Board Member, Bin Cao had no involvement in the peer-review of this article and had no access to information regarding its peer-review. Full responsibility for the editorial process for this article was delegated to Editor Jun Liu.

https://doi.org/10.1016/j.bsheal.2025.05.004
2590-0536/

HIGHLIGHTS

Scientific questions

Community-acquired pneumonia (CAP) is a major global health concern, with limited understanding of longitudinal changes in host gene expression and respiratory microbiome throughout disease progression and recovery.

Evidence before this study

Previous studies have shown that CAP patients exhibit abnormal host responses and microbiota dysbiosis, and that host-microbe interactions are linked to CAP pathogenesis.

New findings

During recovery, CAP patients showed notable changes in immune regulation, coagulation, and mitochondrial function. *Prevotella* declined over time and were positively associated with anti-pathogen and interferon pathways. Host responses and microbiome remained heterogeneous compared to controls even 4 months after infection.

Significance of the study

Dynamic alterations and associations between host transcriptome and respiratory microbiome may promote future mechanistic research and therapeutic development of CAP.

Generally, CAP elicits not only tissue-destructive inflammatory cell infiltration in the airways, but also an acute, robust, and dysregulated systematic host immune response, which can be profiled by high-throughput transcriptome. Several studies have reported that CAP patients have aberrant pro-inflammatory gene expression, interferon pathway activation, and increased anti-pathogenic molecular activity [4–6]. These studies emphasize typical and important gene expression characters of CAP patients, but the rapid and ongoing transcriptional changes with time are neglected. Previous studies also demonstrated the long-term impact of CAP, but mainly focused on clinical symptoms, signs or imaging examination [7–9], little is known about the host gene expression patterns of convalescent patients.

As a factor bidirectionally interacting with pneumonia, the eubiosis of respiratory microbiome has been increasingly emphasized [10]; host-microbe interplay also correlated with immune regulation in the blood [11]. Our previous study also reveals the unique composition of upper respiratory tract (URT) microbiome in severe acute respiratory syndrome coronavirus 2 (SARS-CoV2) pneumonia patients, which even might play a predictive role in the prognosis [12]. Nevertheless, it has not yet been fully determined the changing features of URT microbiome from acute CAP to recovery, the duration of existing disturbance, as well as the potential association between local microbiome and systemic host response.

To this end, we conducted this study to broaden the comprehensive understanding of CAP. We longitudinally collected peripheral blood and oropharyngeal swabs of CAP patients for host response and respiratory microbiome analysis. We proceeded with the follow-up approximately 4 months after discharge and performed integrated analyses of systemic transcriptome and URT microbiome. Through this approach, we aimed to elucidate the dynamic interplay between host responses and oropharyngeal microbiome alterations throughout the disease course and recovery, and to identify potential targets for promoting complete restoration of health in CAP patients.

2. Materials and methods

2.1. Study design

Longitudinal samples including peripheral blood and oropharyngeal swabs were collected after CAP patient admission within 24 h (admission status, annotated as T1), a second collection 2–3 days later (median phase of CAP hospitalization, T2), and within 48 h before discharge (improved status, T3). Follow-up was conducted approximately 4 months post infection (convalescence, T4) without any respiratory symptoms reported by participants. CAP was diagnosed according to guidelines of the Infectious Diseases Society of America and the American Thoracic Society [13]. CAP patients with CURB-65 score [14] ≤ 2 (low or intermediate mortality risk) were recruited since we focused more on the recovery process of patients. Meanwhile, age- and sex-matched volunteers who reported no respiratory symptoms and no use of antibiotics in the past 4 weeks were recruited as healthy controls.

2.2. Sample collection

Approximately 2 mL whole blood was collected into PAXgene Blood RNA tubes (BD, New York, USA) and placed at room temperature, incubated for 30 min and then transferred to -20°C for storage. Whole blood for extracting peripheral blood mononuclear cells (PBMCs) were collected in ethylenediaminetetraacetic acid-anticoagulated tubes (BD). Oropharyngeal swab (Copan, Brescia, Italy) samples were aliquoted into tubes within 8 h after being collected and subsequently frozen at −80 C until extraction.

2.3. Targeted next-generation sequencing for pathogen detection

Targeted next-generation sequencing (tNGS) of sputum collected after initial admission (oropharyngeal swabs as an alternative for those patients who did not have sputum) was conducted in all CAP patients for pathogen detection. Respiratory Pathogen Detection Kit (KingCreate, Guangzhou, China) was used following the manufacturer's protocol. Ultra-multiplex polymerase chain reaction (PCR) amplification was performed using the pathogen panel listed in Table S1. A positive control and a negative control were set up during the process. Qualified library was sequenced on an Illumina MiniSeq platform.

2.4. RNA extraction, library preparation, and sequencing

Total ribonucleic acid (RNA) was extracted by the PAXgene Blood RNA Kit (Qiagen, Hilden, Germany) according to manufacturer's instructions. The concentration and integrity of total RNA were assessed by RNA Nano 6000 Assay Kit of the Bioanalyzer 2100 system (Agilent Technologies, Santa Clara, USA). Sequencing libraries were conducted using the TruSeq RNA Library Prep Kit (Illumina, San Diego, USA). The quality of libraries was measured by Agilent 2100 bioanalyzer (Agilent Technologies) and the final library pool concentration was determined using KAPA Library Quantification Kits (Roche, Basel, Switzerland). Libraries were sequenced by Illumina NovaSeq 6000 platform to generate 150 base pairs paired-end reads.

2.5. DNA extraction, library preparation and sequencing

The total respiratory bacteria DNA was extracted from oropharyngeal swab samples by MagMAX Microbiome Ultra Kit (Thermo Fisher, Waltham, USA). The quantity and quality were then measured by the NanoDrop NC2000 spectrophotometer (Thermo Fisher) and agarose gel electrophoresis, respectively. PCR amplification of the bacterial 16S ribosomal ribonucleic acid (rRNA) genes V3–V4 region was performed using the forward primer 338F (5′-ACTCCTACGGGAGG CAGCA-3′) and the reverse primer 806R (5′-GGACTACHVGGGTWTC TAAT-3′) and barcodes were incorporated into the primers for multi-

plex sequencing. PCR products were purified and quantified by the Quant-iT PicoGreen dsDNA Assay Kit (Invitrogen, Carlsbad, USA). Amplicons were pooled and then sequenced on an Illumina NovaSeq 6000 platform. Three deoxyribonucleic acid (DNA) extraction controls and three PCR amplification controls failed the quality control before sequencing due to the lower concentration of purified products than the detection threshold.

2.6. Transcriptome analysis

Raw RNA-sequencing reads were quality-controlled by Fastp 2.1.0. HISAT2 2.1.0 was used to map filtered clean data to human genome GRCh38.109. Gene expression counts were finally obtained by featureCounts 1.5.0-p2. Subsequent analyses were performed in R 4.3.0. EdgeR 4.0.1 was used for normalization and differential analyses. Differentially expressed genes (DEGs) were defined as the adjusted P value <0.05 (Benjamini-Hochberg method) and absolute fold change >2, followed by visualized using volcano plots. For time series analysis, Mfuzz [15] 2.62.0 was used. The all Gene Ontology (GO) functional analyses were performed by clusterProfiler [4] 4.10.0 and visualized by ggplot2 3.4.4. Gene set enrichment analysis (GSEA) was performed using clusterProfiler [16] 4.10.0 and visualized by ggplot2 4.10.0 or GseaVis 0.1.0. The Hallmark gene sets were downloaded from Molecular Signature Database (MSigDB). In addition, the proportions of immune cells in blood were speculated by Cell-type identification by estimating relative subsets of RNA Transcripts (CIBERSORT) [17] algorithm 1.06 based on the transcripts per million (TPM) of genes. Pathway-level information extractor (PLIER) [18], was then used to summarize the activation and inhibition of pathways. The package decomposed gene expression data into several latent variables (LVs), which were further automatically matched to the most relevant pathways based on prior knowledge. LVs which were annotated as known immune-related biological functions were displayed.

2.7. Isolation of PBMCs and detection of cellular ATP content

Peripheral blood mononuclear cells (PBMCs) obtained from CAP patients and controls were isolated using standardized Ficoll methods. After final wash, the cell pellet was resuspended with CS10 cryopreservation medium (STEMCELL, Vancouver, Canada) and then placed in a freezing container at -80 °C. After thawing, PBMCs were resuspended in Roswell Park Memorial Institute (RPMI) 1640 medium (Thermo Fisher) supplemented with 10 % Fetal Bovine Serum (FBS) (Thermo Fisher) and 1 % Penicillin-Streptomycin (Thermo Fisher), and then counted and seeded at a density of 2×10^6 cells/mL in ultra-low attachment U-bottom 96-well plates (Corning, Corning, USA). After resting overnight at 37 C in a 5 % CO_2 incubator, luminescent adenosine triphosphate (ATP) detection assay (DOJINDO, Kumamoto, Japan) was conducted according to the manufacturer's instructions.

2.8. Microbiome analysis

The 16S rRNA amplicon sequencing bioinformatics analysis was performed with a pipeline from EasyAmplicon [19] 1.19 in R 4.3.0 with slight modification. Briefly, raw data were filtered by vsearch 2.23.0 to remove primers, barcodes and low-quality reads with parameters: fastq_stripleft 29, fastq_stripright 18 and fastq_maxee_rate 0.01. Clean amplicons were then denoised into amplicon sequence variants (ASVs) in de novo mode and mapped to the Ribosomal Database Project (RDP) 11. 19,065,691 (84.49 %) sequences were successfully mapped. In addition, alpha- and beta-diversity metrics were calculated using an even sampling depth of 40,000 sequences per sample from Vegan 2.6–4 and visualized by ggplot2 3.4.4, as well as the community histogram plot. Finally, statistical tool of analysing metagenomic profiles (STAMP) [20] 2.1.3 were used to detect differential microbes at various levels.

2.9. Integrated analysis of microbiome and transcriptome results

Weighted gene co-expression network analysis (WGCNA) was conducted using the top 6,000 genes with high Median. Representative blood routine examination results (white blood cell count, neutrophil count, platelet count and lymphocyte count) and the relative abundance of differential genera ($P < 0.05$) identified by STAMP (*Haemophilus*, *Neisseria*, *Porphyromonas* etc.) were used as input traits of CAP patients and controls. After constructing the weighted adjacency matrix, a topological overlap matrix (TOM) was formed. Gene co-expression modules were identified by the dynamic cut-tree algorithm. GO enrichment analyses and visualization were performed as described above. Kyoto Encyclopedia of Genes and Genomes (KEGG) enrichment was performed by clusterProfiler 4.10.0 and visualized by ggplot2 3.4.4.

2.10. Availability of data

The raw sequence data reported have been deposited in the Genome Sequence Archive in National Genomics Data Center, China National Center for Bioinformation / Beijing Institute of Genomics, Chinese Academy of Sciences under CRA007003 for RNA sequencing at https://ngdc.cncb.ac.cn/gsa-human and CRA015487 for 16S rRNA sequencing at https://ngdc.cncb.ac.cn/gsa, respectively.

3. Results

3.1. CAP patients showed distinct transcriptional profiles during hospitalization, and persisted up to 4 months after discharge

Our cohort consisted of 44 CAP patients and 44 matched non-infectious healthy controls (HCs) (Fig. 1A). The median age (Q1, Q3) of patients was 66.5 (57.8, 76.0) years old and that of HC was 64.5 (58.0, 68.0) ($P = 0.176$). Male participants accounted for 54.5 % in patients and 40.9 % in controls ($P = 0.286$). For pathogen detection, 33 (75.0 %) patients were demonstrated positive results by targeted Next-Generation Sequencing (tNGS), among which patients with a virus infection occupied 27.3 %, respectively. Six patients (13.6 %) were identified as mono bacterial infection. Other infection types were identified in one patient (2.3 %), respectively. Detailed demographic and clinical features of participants were shown in Table 1. For transcriptome analyses, we collected a total of 164 transcriptome samples (peripheral blood) from patients with CAP (n = 120) and control subjects (n = 44). The samples from CAP patients were distributed as follows: 34 samples at time point T1, 32 samples at T2, 38 samples at T3, and 16 samples at T4. Meanwhile, we obtained 44 samples from control subjects. For microbiome analyses, we obtained samples (oropharyngeal swab) from the CAP group as follows: 40 samples at T1, 37 samples at T2, 36 samples at T3, and 15 samples at T4; and 44 samples from the control group.

Initial analyses of the data indicated significant differences in gene expression profiles at all time points compared to HCs (Fig. 1B). The differentially expressed genes (DEGs) were different but partially overlapped compared to HC during the four observation stages (Fig. 1C-1E). We obtained 1,327 up-regulated and 1,133 down-regulated genes at CAP baseline, and even more, 1,415 up-regulated and 2,357 down-regulated DEGs before discharge. While for patients in follow-up, 1,033 and 183 genes were still considered significantly up- or down-expressed compared to HC (Fig. 1C). Notably, the top DEGs such as *MPO*, *MMP8*, *BEX1*, *PRTN3*, *LTF* remained at high levels even 4 months post infection, whereas *HBM*, *VMO*, *RPS29*, *HBQ1*, etc. showed the opposite expression trend (Fig. 1E). In summary, we found persistently perturbed and complicated expression profiles during disease course. Despite the disparities minimized over the course of the follow-up, the systematic transcriptomic profile of patients with CAP continued to differ from that of controls 4 months post CAP.

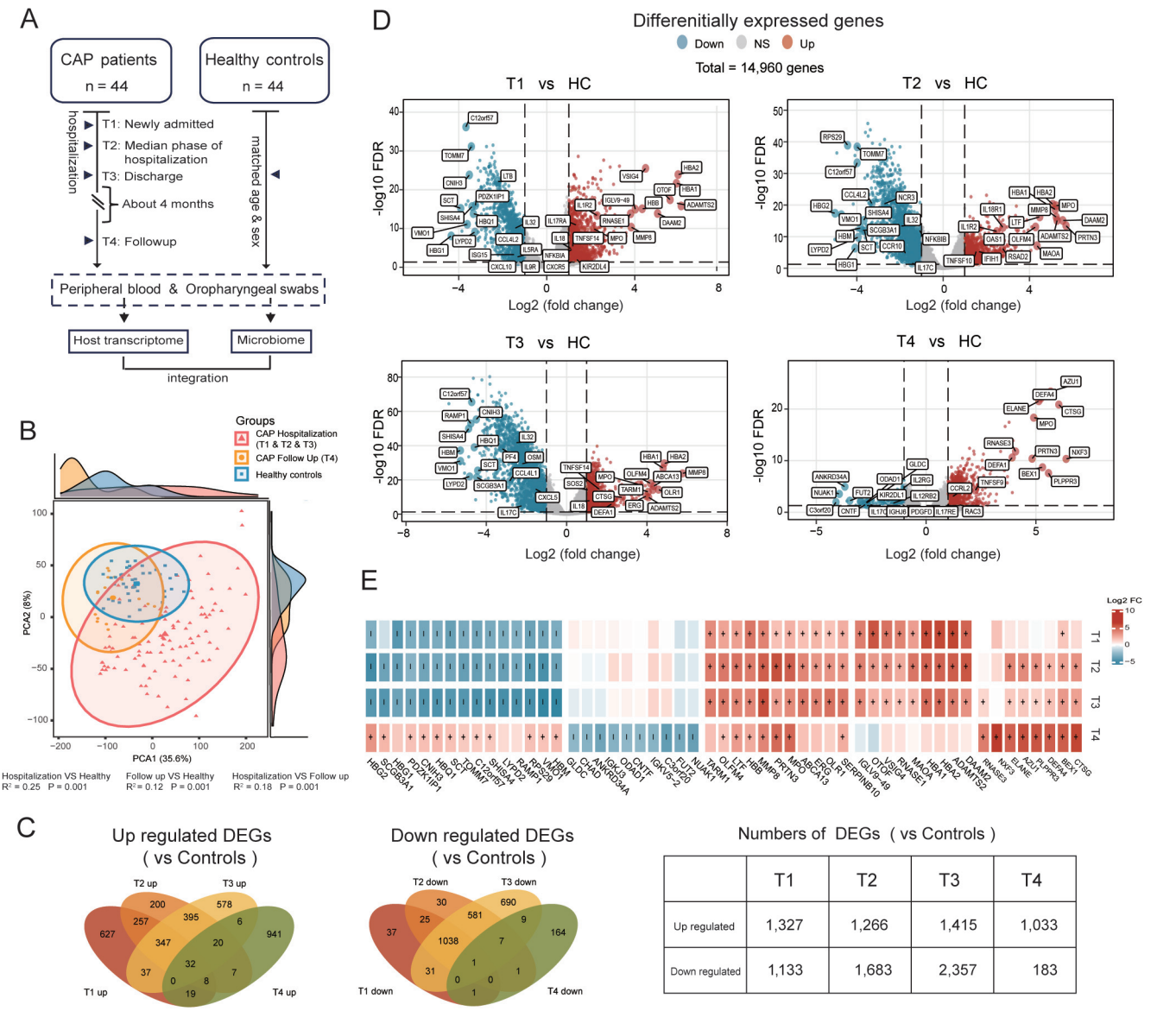

	T1	T2	T3	T4
Up regulated	1,327	1,266	1,415	1,033
Down regulated	1,133	1,683	2,357	183

Fig. 1. Identification of DEGs in CAP patients. A) Study design. Peripheral blood and oropharyngeal swabs were collected from patients at four timepoints. Samples from healthy people were served as controls. B) PCA plot showed significant difference on gene expression profiles among groups (PERMANOVA test or pair-wise PERMANOVA test). C) Venn diagrams of up or down regulated DEGs between CAP versus controls and detailed numbers. T1, admission status; T2, median phase of CAP hospitalization; T3, improved status; T4, convalescence. D) Volcano plots of DEGs per sampling timepoint. The names of protein-coding or immune-related genes with the top absolute FC were labelled. E) Heatmap of expression levels of top 10 protein-coding DEGs at different timepoints vs. healthy control group. "+" or "-" represented significantly upregulated or downregulated. For differential expression, $|FC| > 2$ and FDR < 0.05 were selected. Abbreviations: CAP, community-acquired pneumonia; DEG, differentially expressed gene; FC, fold change; FDR, false discovery rate.

3.2. Temporal transcriptomic analysis reveals striking alterations during the recovery from CAP

We further clustered DEGs according to their expression patterns, and then performed functional enrichment analysis since we thought the trajectories of them were ultimately reflected by the pathway functions. Fig. 2A represented a group of genes showing "up-stable-down" trend (*BCL6*, *MYD88*, *STAT6*, *IGLC2*, *IGHA1*, *OAS1*, etc.). They were consistently overexpressed during hospitalization, but down-regulated after discharge. They were significantly enriched in immune responses pathways, characterized by "B cell mediated immunity" ranking first among all GO terms, suggesting the differentiation and activation of adaptive immune cells were rather active during hospitalization. Furthermore, genes in cluster 2 (*VWF*, *GP6*, *F13A1*, *PEAR1*, *F2RL3*, *MPIG6B*, etc.) displayed "up-down-down" trajectory, characterized by marginal decline during the acute phase and sharp decline after discharge (Fig. 2B). The top enriched pathways contained "blood coagulation", "hemostasis", and "platelet activation", indicating robust coagulation disorders in CAP patients initially, though it returned to homeostasis gradually (Fig. 2B). By contrast, cluster 3 (*NDUFB1*, *NDUFB2*, *ATP5MG*, *ATP5F1E*, *COX7A2*, *UQCR11*, etc.), showing "down-down-up" trend, represented DEGs with continuous down-regulation during the hospitalization but increasing expression thereafter (Fig. 2C). One prominent feature of these genes was that they were involved in the mitochondrial structure and functional pathways, such as "oxidative phosphorylation", "mitochondrial adenosine triphosphate (ATP) synthesis coupled electron transport", and "mitochondrial respiratory chain complex I assembly", suggesting the temporary abnormal energy metabolism (Fig. 2C). To characterize the internal dynamic features of CAP patients at different timepoints, we

Table 1
Baseline characteristics of enrolled patients and controls.

Demographics	CAP patients (n = 44), n (%)	Controls (n = 44), n (%)	*P* value
Sex (male), n (%)	24 (54.5)	18 (40.9)	0.286
Age (years), median (Q1, Q3)	66.5 (57.8, 76.0)	64.5 (58.0, 68.0)	0.176
Current smoke[a], n (%)	4 (9.0)		
Pathogen detected[a,b], n (%)			
Virus only	12 (27.3)		
Bacteria only	6 (13.6)		
Fungus only	1 (2.3)		
Mixed infection	14 (31.8)		
Undetected	11 (25.0)		
Comorbidity[a], n (%)			
Respiratory diseases[c]	2 (4.5)		
Cardiovascular diseases[d]	18 (40.9)		
Type 2 diabetes mellitus	3 (6.8)		
Blood routine examination ($\times 10^9$/L)[a], median (Q1, Q3)			
White blood cell count	5.5 (4.4, 7.0)		
Neutrophils	4.0 (3.1, 5.1)		
Lymphocytes	1.0 (0.8, 1.4)		
Platelet	219.0 (167.5, 255.5)		
Antibiotic therapy[a], n (%)	36 (81.8)		
Hospital stay (days)[a], median (Q1, Q3)	6.9 (5.0, 8.5)		
90-day mortality[a], n (%)	0 (0)		
CURB-65[a,e]	1 (0–1)		

Data are presented as median (interquatile range Q1, Q3) or n (%).
[a] Healthy individuals do not have these indicators.
[b] Pathogens detected by targeted next-generation sequencing (tNGS) using sputum or oropharyngeal swab (for those patients who did not have sputum). The list of 198 pathogens was shown in Table S1.
[c] Bronchiectasis or chronic bronchitis.
[d] Hypertension or coronary artery diseases.
[e] The CURB-65 score is a clinical prediction tool used to assess the severity of community-acquired pneumonia, including the following indicators: Confusion (C), Urea (U), Respiratory rate (R), Blood pressure (B), and age ≥65 years (65).

directly compared the expression and enrichment of DEGs from T3, T4 compared to T1, the top pathways of which resembled with the above enriched pathways (Fig. 2D, 2E). We further displayed the representative gene set enrichment analysis (GSEA) results comparing patients and healthy controls to corroborate our observations (Fig. 3A). “Oxidative phosphorylation”, “coagulation”, and typical immune-related pathways fluctuated during the observation phase (Fig. 3A). To validate the dysregulation of mitochondrial energy metabolism detected by pathway enrichment, we used the peripheral blood mononuclear cells (PBMCs) in the whole blood from some participants (Table S2) to detect the cellular ATP contents, a direct indicator to evaluate the mitochondrial function. The lower levels of cellar APT in PBMCs from hospitalized CAP patients demonstrated impaired function on energy production at acute phase (Fig. 3B). Overall, we observed complex transcriptional variations of CAP compared to HCs, in which immune modulation, coagulation system and energy metabolism were the most striking alterations.

3.3. Long-term alterations of CAP patients' immune expression profiles

To illustrate the immune scenarios of CAP patients, we firstly calculated the proportion of nine main immune cells (Fig. 4A) speculated by cell-type identification by estimating relative subsets of RNA transcripts (CIBERSORT), followed by assessment of the abundance of 22 cell subtypes (Fig. 4B, Fig. S1). During the observation phase (T1 to T4), Tregs were consistently and significantly different between CAP patients and controls. Their levels continued to decline during hospitalization but restored after discharge, despite not to normal (Fig. 4B). In the whole acute phase of CAP (T1 to T3), we observed several notable immune cell abnormalities, including an increase in activated cluster of differentiation 4 ($CD4^+$) memory T cells and a decrease in $CD8^+$ T cells and natural killer (NK) cells, while their proportions returned to normal during the follow-up stage (Fig. 4B). Additionally, CAP patients exhibited higher percentages of neutrophils and M2 macrophages at T2 and T3, but not at the initial stage of hospitalization (T1), and then persisted even after discharge (T4) (Fig. 4B).

In addition to cell components, we used pathway-level information extractor (PLIER), to detect activation or suppression of immune-related pathways. We showed 20 latent variables (LVs) which could be annotated as known immune pathways in databases (Fig. 4C). Other pathways identified by PLIER, mainly related to metabolism and blood function were displayed in Fig. S2. The changes in some critical processes, such as apoptosis (LV52, LV72), endocytosis (LV114), Fc gamma receptor mediated phagocytosis (LV22), NK cell mediated cytotoxicity (LV73) demonstrated continuous remodeling of the immune system in CAP patients. In similar, significant dynamic adjustment in humoral immunity, e.g. antigen processing ubiquitination proteasome degradation (LV103), and cellular immunity, e.g. $CD8^+$ T Cell Receptor (TCR) downstream pathway (LV61) were significantly involved (Fig. 4C). Besides, the gene expression of some cytokines or their receptors, such as *IL7*, *IL18*, *CCL3*, *RANTES*, *IL17RC*, etc. were dysregulated (Fig. 4D). Note that many modifications terminated in moderation at T4 (statistically not significant at T4) (Fig. 4C). These observations suggested that the immune microenvironment showed rapid, dynamic and moderate responses against CAP at the levels of cell proportions and functional pathways.

3.4. URT microbial diversity and composition changes with time

Besides the systemic transcriptomic changes observed above, the upper respiratory tract microbiome also exhibited dynamic variations. We collected oropharyngeal swabs from both patients and healthy control subjects, which were subsequently analyzed using 16S rRNA (ribosomal Ribonucleic Acid) sequencing. The alpha diversity and microbiome composition were compared between the two groups. Alpha diversity, which represents the internal diversity within a specific sample, was assessed using several indices. The richness index, abundance-based coverage estimator (ACE) index and Chao1 index were significantly lower in the patient group compared to the control group at all time points (Fig. 5A). Similarly, the Shannon index showed significant differences, except at T1 and T4 (Fig. 5A, $P < 0.001$), indicating the comparatively homogeneous bacterial composition in patients' URT. The principal coordinates analysis (PCoA) analysis revealed the ecological relationships and differences between the groups. It further indicated patient samples differed significantly from healthy controls ($r^2 = 0.08$, $P = 0.001$) during hospitalization and during follow-up ($r^2 = 0.11$, $P = 0.001$), and also between acute and recovery stage ($r^2 = 0.02$, $P = 0.001$) (Fig. 5B). We then used statistical tool for analysis metagenomic profiles (STAMP) analysis to identify differential microbes at various levels (Fig. 5C, 5D, Fig. 6, Fig. S3). We found that the composition of microorganisms varied between the four timepoints compared to controls: at the phylum level, *Firmicutes* ranked first in CAP patients, while *Bacteroidetes* and *Proteobacteria* were more prevalent in controls (Fig. 5D, Fig. S3); the most abundant genus among all groups was *Prevotella*, though decreasing constantly with time in patients (Fig. 6B). CAP patients and healthy controls showed significant differences and the order of differential genera shifted with time: initially, *Streptococcus*, *Veillonella*, and *Megasphaera* ranked in the top three in patients, while *Streptococcus*, *Gemella,* and *Rothia* were the top 3 abundant genera in convalescent patients and *Veillonella* showed no significance (Fig. 6C, 6D). In summary, we observed CAP patients had long-term respiratory microbiome dysbiosis.

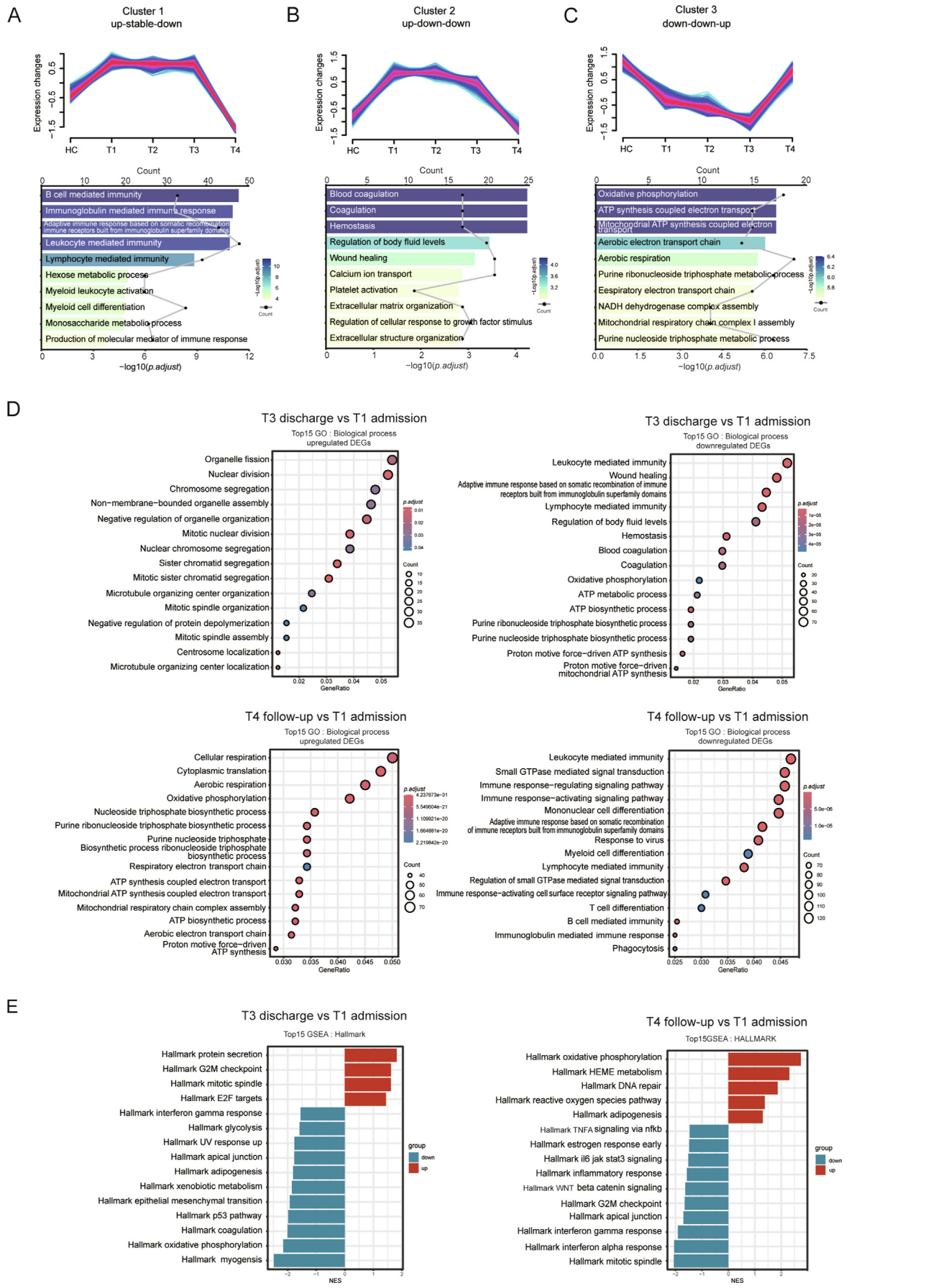

Fig. 2. Longitudinal transcriptomic hallmarks of CAP. A–C) Clustering plots of DEGs expression patterns (top) and top 10 enriched GO terms (bottom). The color of each bar stood for –log10 (adjusted *P* value) (Benjamini-Hochberg method) and dot for enrich count. D–E) Comparison within CAP patients at different timepoints by GO (D) and GSEA enrichment (E) with top 15 pathways shown. T1, admission status; T2, median phase of CAP hospitalization; T3, improved status; T4, convalescence. Abbreviations: CAP, community-acquired pneumonia; DEG, differentially expressed gene; GO, Gene Ontology; HC, healthy control.

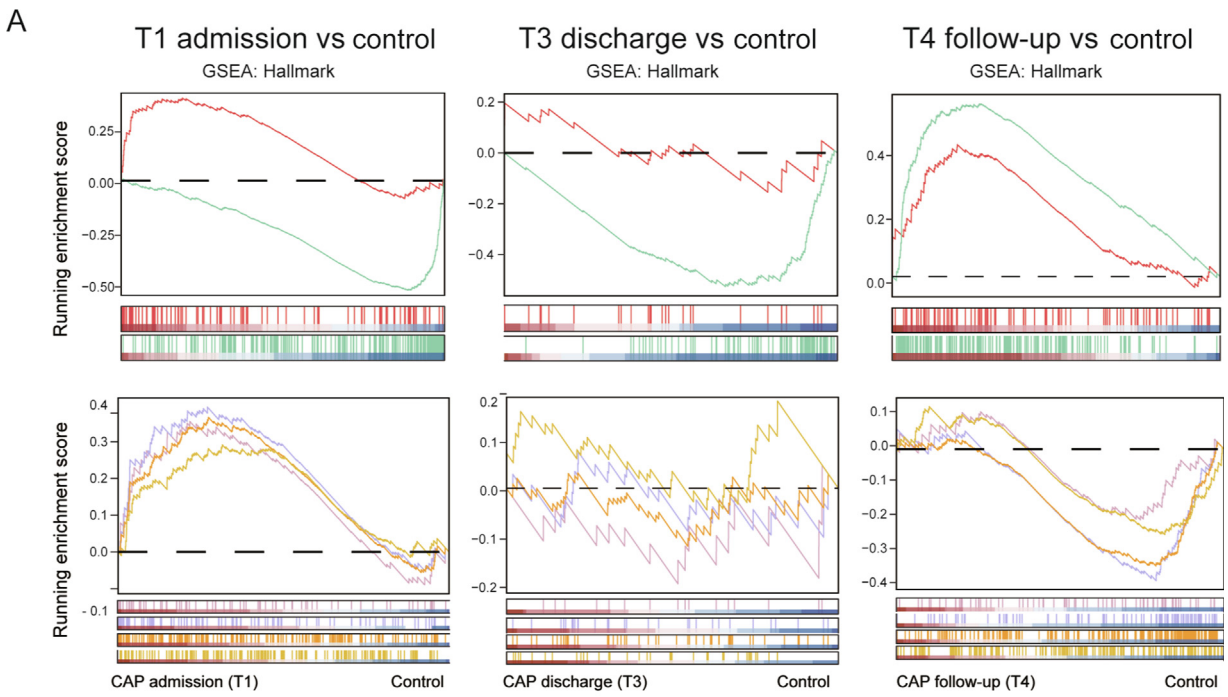

Hallmark term name	T1		T3		T4	
	NES	*p.adjust*	NES	*p.adjust*	NES	*p.adjust*
Oxidative phosphorylation	-2.537	<0.001	2.456	<0.001	2.360	<0.001
Coagulation	1.613	0.011	1.128	0.591	1.622	0.011
Interferon gamma response	1.629	0.002	0.803	0.967	1.669	0.001
Interferon alpha response	1.568	0.009	0.846	0.967	1.678	0.006
Tnfa signaling via nfkb	1.288	0.106	0.827	0.967	1.209	0.218
IL6 jak stat3 signaling	1.364	0.106	0.874	0.931	0.855	1.000

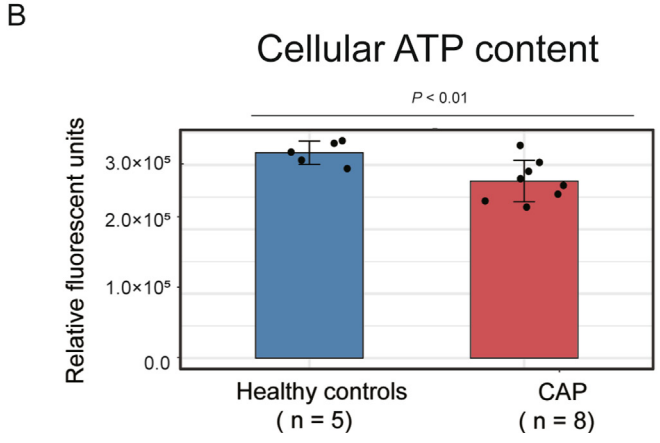

Fig. 3. Representative pathways of CAP. A) GSEA of representative pathways among patients and controls. T1, admission status; T2, median phase of CAP hospitalization; T3, improved status; T4, convalescence. B) Cellular ATP in PBMCs from CAP or controls was measured via a luciferase-based assay and expressed as relative fluorescent units. *P* value was determined using the Mann-Whitney *U* test, showing statistical significance. Error bars showed the mean ± SD. Adjusted *P* value was calculated using Benjamini-Hochberg method. Abbreviations: CAP, community-acquired pneumonia; GSEA, gene set enrichment analysis; PBMCs, peripheral blood mononuclear cells; ATP, adenosine triphosphate; SD, standard deviation; NADH, nicotinamide adenine dinucleotide (reduced form); UV, ultraviolet; GTPase, guanosine triphosphatase; DNA, deoxyribonucleic acid; TNFA, tumor necrosis factor alpha; NFKB, nuclear factor kappa B; IL6, interleukin-6; Jak, Janus kinase; Stat3, signal transducer and activator of transcription 3.

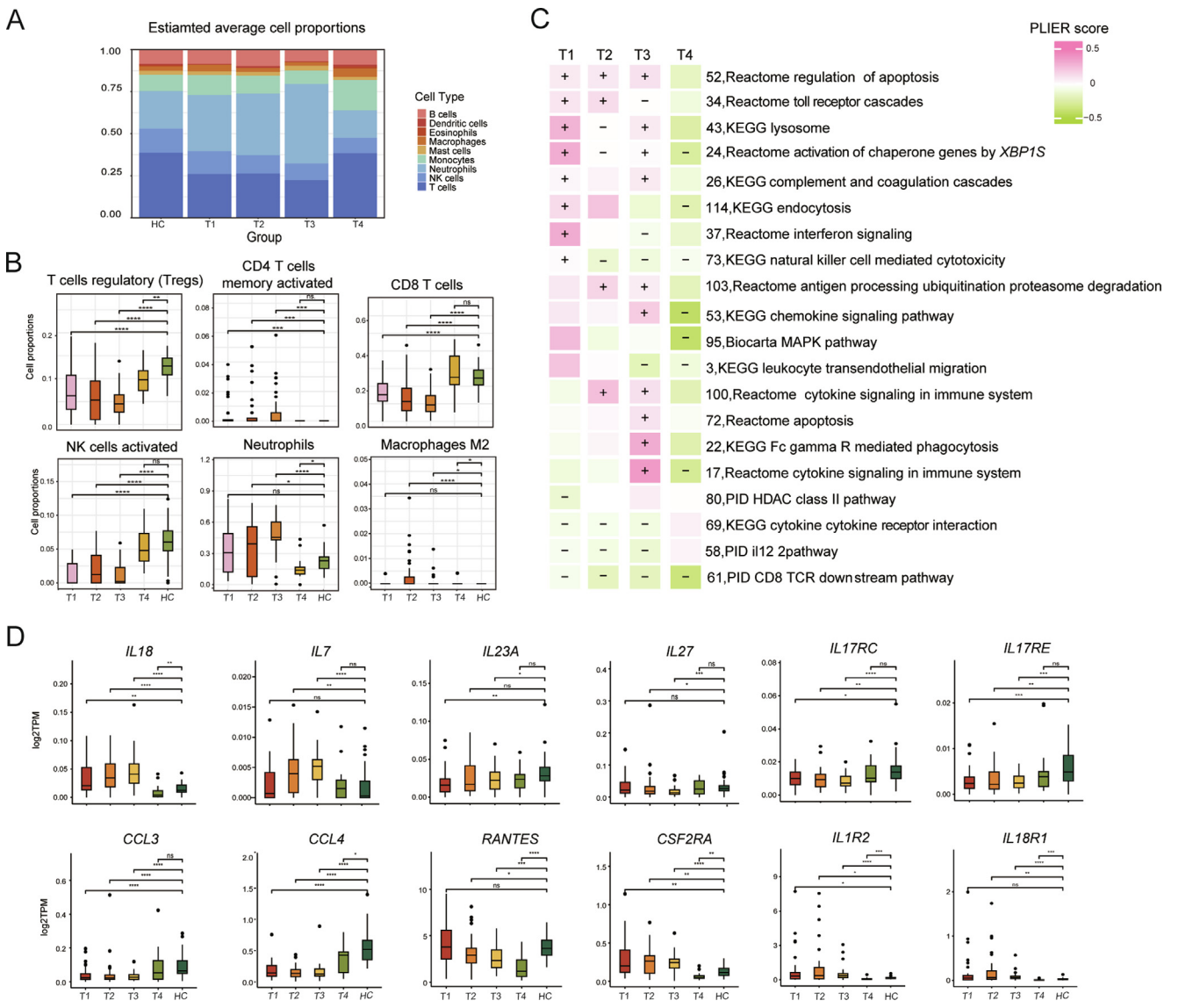

Fig. 4. Dynamic alterations of CAP patients' immune profiles predicted from transcriptome data. A) The proportions of nine major immune cell types. B) Comparison of the representative immune cell proportions between CAP and healthy controls during recovery. C) Heatmap of representative immune-related latent variables with biological function per sampling time. Pathways that were significantly upregulated or downregulated according to the Mann-Whitney *U* test were labeled with "+" or "-", respectively. T1, admission status; T2, median phase of CAP hospitalization; T3, improved status; T4, convalescence. D) Boxplots showed the gene expression of representative cytokines and receptors with time. Mann-Whitney *U* test was used. ns, $P > 0.05$; *, $P \leq 0.05$; **, $P \leq 0.01$; ***, $P \leq 0.001$; ****, $P \leq 0.0001$. Abbreviations: CAP, community-acquired pneumonia; NK, natural killer; CD, cluster of differentiation; KEGG, Kyoto Encyclopedia of Genes and Genomes; MAPK, mitogen-activated protein kinase; PID, pathway interaction database; IL, interleukin; CCL, C-C motif chemokine ligand; CSF, colony-stimulating factor.

3.5. Integrative analyses suggest the associations between URT microbiome and gene transcriptional modules

Based on the observation that the URT microbiome was significantly altered in CAP compared to controls, we hypothesized that these compositional changes, as well as other clinical traits, interplayed with host regulation of transcripts. Thus, we performed weighted correlation network analysis (WGCNA) and then detected a total of seven modules significantly related to various traits (Fig. 7A). We then performed GO and Kyoto Encyclopedia of Genes and Genomes (KEGG) enrichment analyses according to genes in each module (Fig. 7B–7E, Fig. 8). Blue and green modules displayed strong positive correlation with the disease course of CAP and four differential genera (*Haemophilus*, *Neisseria*, *Porphyromonas* and *Stomatobaculum*), whereas negatively correlated to other elements such as white blood cell (WBC) counts, neutrophil (NE) counts and platelet (PLT) counts (Fig. 7A). The GO terms enriched by genes in blue and green modules were overlapped, focusing mainly on mitochondrial structure and function (Fig. 7B); KEGG terms contained "Oxidative phosphorylation" as well (Fig. 8A, 8B). According to our experiment, ATP content in peripheral blood mononuclear cells from CAP patients was lower than that from healthy controls (Fig. 2G), indicating the impaired energy metabolism. Yellow module enriched in the repairment of cell and tissue and signal transduction (Fig. 7C, Fig. 8C), which negatively correlated to disease course (Fig. 7A), indicating active vital remodeling at acute phase. The genes in the red module including *IFIT5*, *IFI6*, *RSAD2*, *MX1*, *MX2*, *etc.* were significantly enriched in antiviral defense, innate immunity and regulation of type I interferon production (Fig. 7D) and in diseases such as "Influenza" and "COVID-19", and pathogen-related receptor recognition pathways (Fig. 8D). Neutrophil counts were positively related to red module, while platelet counts were the opposite (Fig. 7A). *Prevotella*, which was the dominant

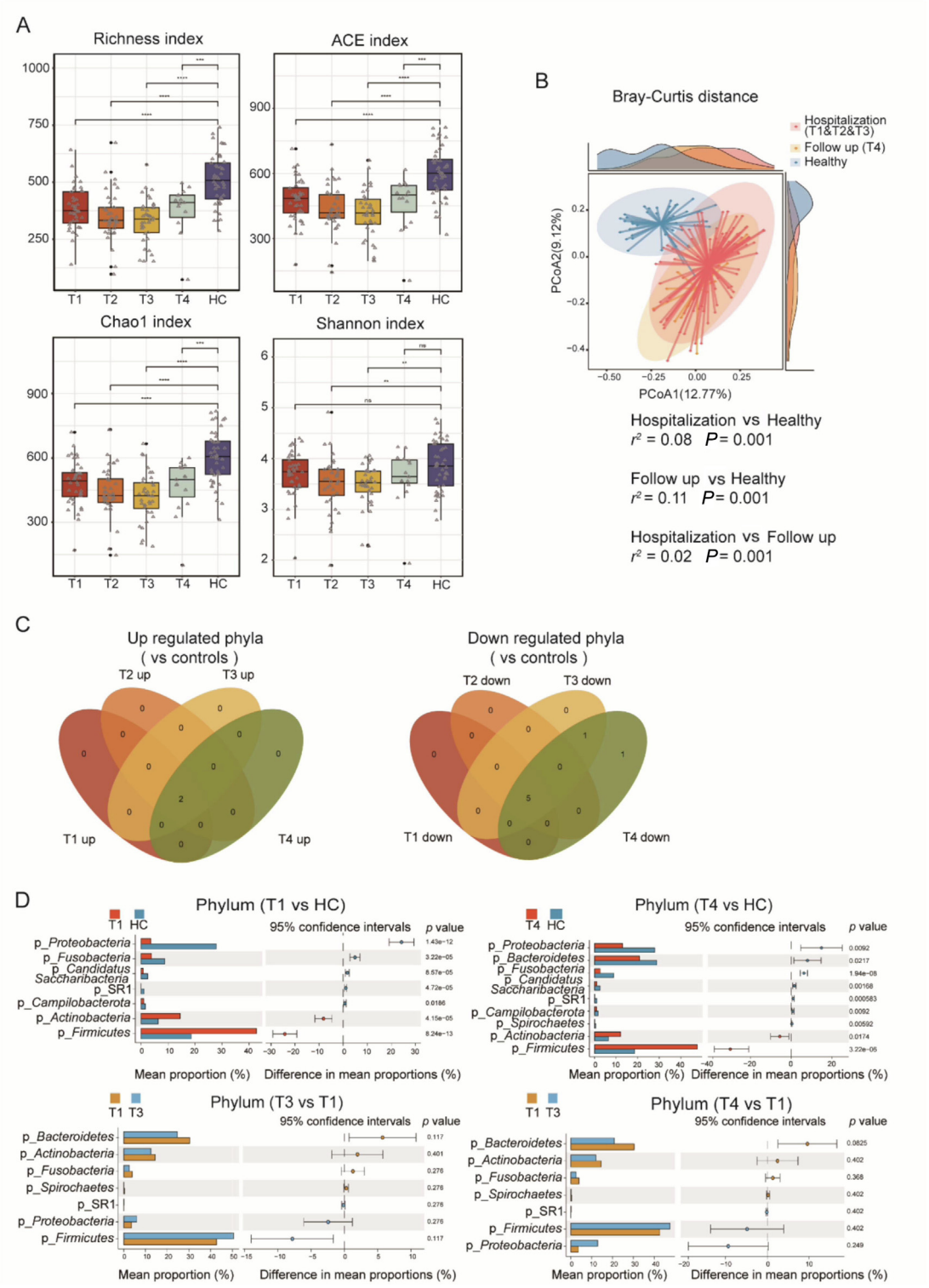

Fig. 5. Respiratory microbiome signatures of CAP during rehabilitation. A) Changes in the α-diversity (genus level) with time. Each triangle represented one swab specimen. B) The β-diversity was assessed by principal coordinates analysis (PCoA) of Bray-Curtis distance. r^2 and significance were shown. PERMANOVA test or pairwise PERMANOVA test was used. C) Venn diagrams summarized the differential phyla of patients compared with controls. D) Detailed results of STAMP analysis at the phylum level. STAMP analysis was performed to distinguish the respiratory microbiome among groups (C–D). T1, admission status; T2, median phase of CAP hospitalization; T3, improved status; T4, convalescence. Abbreviations: CAP, community-acquired pneumonia; PERMANOVA, permutational multivariate analysis of variance; STAMP, statistical tool for analysis of metagenomic profiles; ACE, abundance-based coverage estimator; HC, healthy control.

genus in URT and enriched in non-infectious controls (Fig. 6B, 6C), was the only genus significantly correlating to red module (r^2 = 0.35, P = 0.001) (Fig. 7A). Brown and turquoise module enriched in the nucleotide metabolism and protein modification (Fig. 7E, Fig. 8E and 8F), indicating an active synthesis and degradation, showing positive association with the relative abundance of

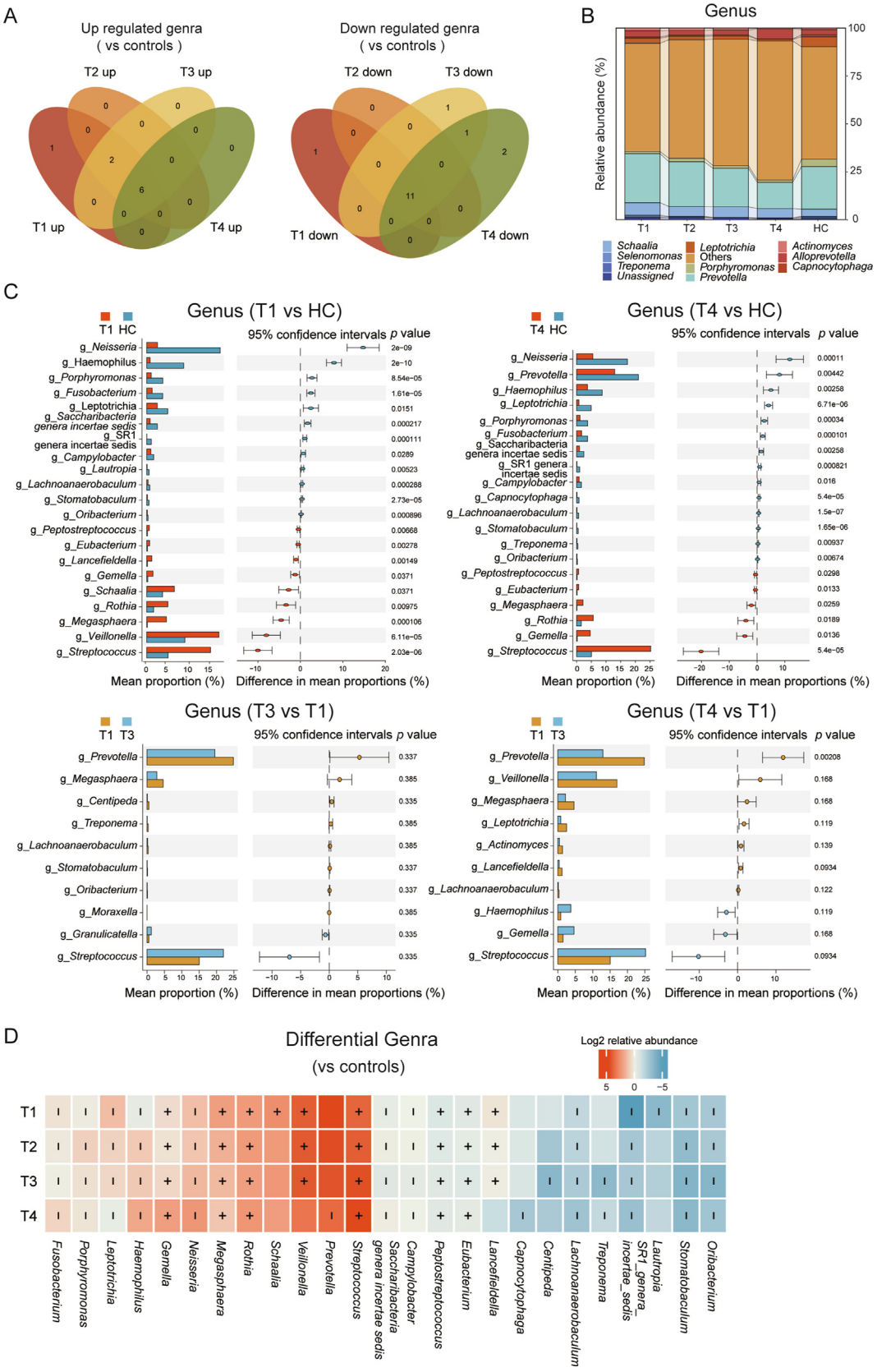

Fig. 6. Respiratory genus signatures of CAP during rehabilitation. A) Venn diagrams summarized the varied genera. B) Histogram displayed the microbial compositional profiling. C) Detailed STAMP analysis results at the genus level. D) Heatmap of differential genera. STAMP analysis was performed to distinguish the respiratory microbiome among groups (A–D). Mann-Whitney *U* test was used and significantly upregulated or downregulated genera were labelled with "+" or "-". T1, admission status; T2, median phase of CAP hospitalization; T3, improved status; T4, convalescence. Abbreviations: CAP, community-acquired pneumonia; STAMP, statistical tool for analysis of metagenomic profiles; ACE, abundance-based coverage estimator; HC, healthy control.

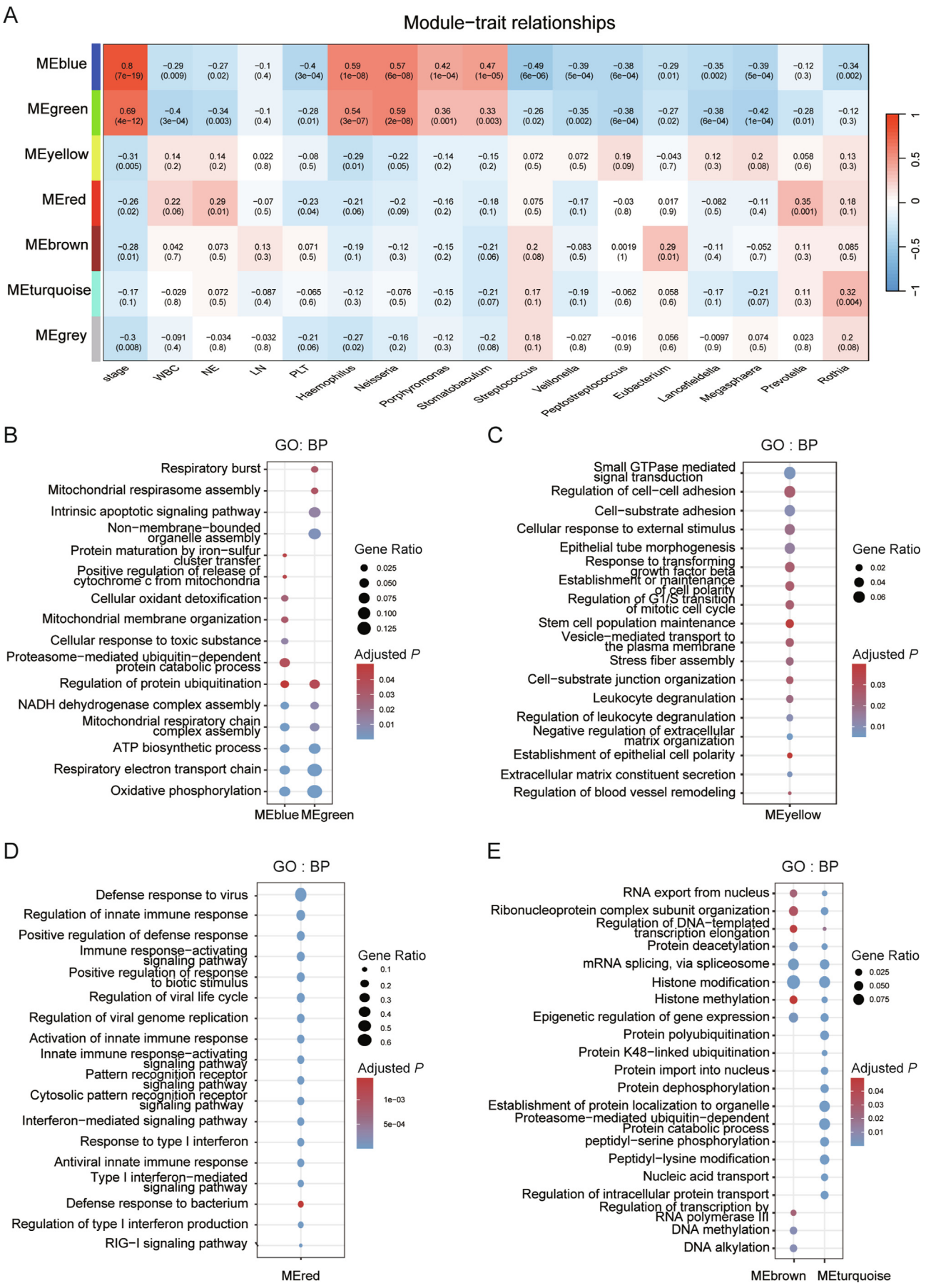

Fig. 7. WGCNA indicated the relationship between host transcriptome and microbiome. A) Correlations between WGCNA gene modules, clinical traits, and relative abundance of differential respiratory microbes. The correlation coefficient and adjusted *P*-value (in parentheses) were provided. Adjusted *P* value was calculated using Benjamini-Hochberg method. B–E) GO gene enrichment analysis for each module. The size of the bubble represented enriched GO gene ratio. Representative pathways were shown. Abbreviations: GO, gene ontology; BP, biological process; WGCNA, weighted correlation network analysis.

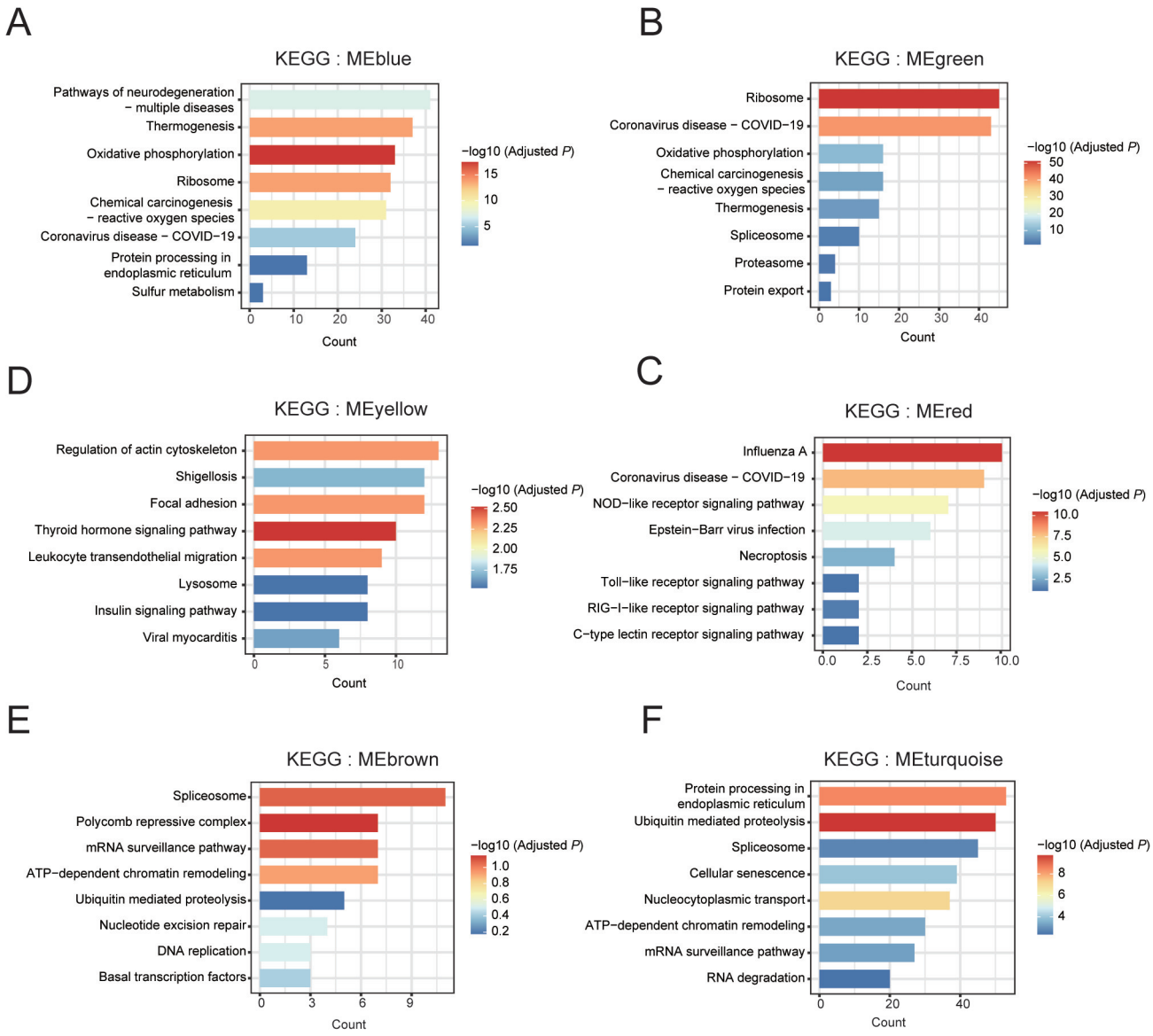

Fig. 8. WGCNA indicated the relationship between host KEGG pathway and microbiome. A–F) KEGG analysis for modules. Representative pathways were shown. The colors of the bars (A–F) represented the -log10 (adjusted *P*) (Benjamini-Hochberg method). Abbreviations: WGCNA, weighted correlation network analysis; KEGG, Kyoto Encyclopedia of Genes and Genomes; NADH, nicotinamide adenine dinucleotide (reduced); ATP, adenosine triphosphate; GTPase, guanosine triphosphatase; RIG-I, retinoic acid-inducible gene I; DNA, deoxyribonucleic acid; RNA, ribonucleic acid; mRNA, messenger RNA; COVID-19, coronavirus disease 2019.

Rothia, *Eubacterium,* and *Streptococcus* (Fig. 7A). Overall, the observations revealed that various both clinical traits and microbial compositions impacted on the host transcriptome, and the associations between them might play a role during the recovery from CAP.

4. Discussion

In this study, we presented the longitudinal landscape of transcriptional and microbial profiles and their mutual associations in CAP patients. Our results demonstrated that the dynamic and complex gene expression perturbations and altered respiratory microbiome structures, persisted for at least 4 months post-infection, with gene expression differences diminishing faster than microbial changes.

Transcriptomics has enhanced our understanding of infection from the perspective of molecules and their function [4–6]. Our study expands previous studies by multiple timepoint profiling of host response from acute phase to the convalescent stage. We found some vital immune regulatory genes such as *MPO*, *MMP8,* and *LTF* remained high expression during the whole observation period, indicating long-term modulation post infection (Fig. 1E). We also found three striking transcriptional events changed during recovery: immune modulation persisted (Fig. 2A, 2D, and 2E; Fig. 3A; Fig. 4C, 4D); hematopoietic function (Fig. 2B, 2D, and 2E; Fig. 3A) and metabolic process (Fig. 2C, 2D, and 2E; Fig. 3; Fig. S1) gradually tended to normal from acute CAP to recovery. The moderate activation of the immune system, consisting of the collaborative cooperation of exogenous stimuli, immune cells, cytokines, *etc.*, obviously contributes to the clearance of community-acquired pathogens, which also explains why immunosuppressed patients usually have higher morbidity and lower survival rate in infectious diseases [21,22]. However, hyperactivation of the immune response may cause damage via “cytokine storm” [23] or other mechanisms, which could be a predictor of poor outcome in COVID-19 [24] and influenza [25]. Thus, our results emphasize the importance of an active immune response and, more importantly, the timely initiation and proper termination of this response.

Infection and inflammation have been widely recognized as a trigger for platelet activation and thrombosis [26,27]. M. Falcone et al. [28] have demonstrated the clinical benefits of aspirin (an anti-

platelet aggregation drug) intake by CAP patients; the monocytes of COVID-19 patients displayed a pro-thrombotic signature [29]; patients in our cohort also showed disturbed pathways related to the blood system such as coagulation and platelet activation (Fig. 2B, 2D, 2E; Fig. 3A). It would be valuable to strike a balance in the inflammatory milieu — between benefiting from moderate platelet activation, such as preventing the spread of pathogens [26], and suppressing excess coagulation [26,27].

CAP patients admitted to general wards displayed an energy metabolism impairment feature (Fig. 2C, 2D, and 2E; Fig. 3; Fig. S1) and the ATP contents in their PBMCs were significantly lower than those from controls (Fig. 3B). In a sepsis cohort (CAP as primary infection), P. Severino et al. [30] proposed a gene set related to oxidative phosphorylation assisting predicting clinical outcomes. We speculated many pathogens or inflammatory factors interfered with host metabolism. Therefore, therapies aiming at maintaining metabolic stability might benefit CAP patients [31]. Taken together, our study indicates the dynamic and complicated variation of gene expression profiles during CAP phase. The imbalance of any aspect of the triangle — immune modulation, hematological system, and metabolism — may cause a vicious cycle [26,27,31].

Pneumonia occurs when the human immune system fails to effectively combat the rapid expansion of pathogens. Despite utilizing tNGS, a broad-coverage pathogen detection method, we were still unable to identify pathogens in 11 patients. This may be due to a low pathogen load or the presence of rare or mutated pathogens not covered by our targeted detection approach. The microbiome of the respiratory tract serves as a vital gatekeeper and plays multiple roles in the shift between health and disease [10,32–34]. The determinants of lung microbiome formation remain elusive, while several studies have demonstrated that the nonnegligible role of the microbiome in the oral cavity and upper respiratory tract [35,36]. Our previous study analysed the correlation between URT microbiome and mortality of COVID-19 pneumonia and found the high temporal stability and protective potential of *Streptococcus*-dominated microbiome [12]. Given that the oropharyngeal swab is an easily accessible specimen for participants, we sampled at four timepoints to document the detailed profiles of respiratory microbiome from acute phase to recovery stages, which is one of the highlights of our study. We observed noticeable shifts of dominant microbes at different levels in CAP patients (Fig. 5C, 5D; Fig. 6). Currently, there is no accepted therapy targeting respiratory dysbiosis, though various probiotics or prebiotics have shown benefits in digestive infectious diseases by promoting the self-barrier formation in the digestive tracts [37,38]. We propose that further exploration is needed to determine whether microecological therapies could benefit respiratory infections [32,38].

We further integrated the host response and local microbiome (Fig. 7A) and discovered that several genera are related to host functional modules. Specifically, the *Haemophilus*, *Neisseria*, *Porphyromonas*, *etc.* are positively related to mitochondrial structure and function process (Fig. 7A, 7B; Fig. 8A, 8B). CAP decreased the relative abundance of *Prevotella*, which showed positive association with genes enriched in viral infection defense and interferon signaling pathways (Fig. 7A, 7D; Fig. 8D). Interestingly, species in *Prevotella* spp. play complex roles [39]: some species lead to pulmonary infections [40], but *Prevotella histicola* and *Prevotella nigrescens* have recently been demonstrated to combat *Pseudomonas aeruginosa* in a cystic fibrosis bronchial epithelial cell model [41].

Our study has several limitations. Firstly, patients enrolled in this study are mainly elderly (median age: 66.5 years) with a limited sample size. This indicates that the results should be validated in a younger patient population with larger cohorts. In terms of microbiome analysis, 16S rRNA amplicon sequencing is not precise enough to detect the alterations of microbiome at species or strains level. Future studies should use the optimal specimen from lower respiratory tract such as sputum and bronchoalveolar lavage fluid to disentangle the dynamic changes of microbiome by metagenomic sequencing.

To sum up, it may be beneficial to pay attention to the coagulation function and energy metabolite dysbiosis in CAP patients, as well as to implement appropriate therapies to prevent abnormal or excessive immune responses, which play a crucial role in facilitating pneumonia recovery. Given the persistent microbiome dysbiosis in the respiratory tract during CAP, future research on microecological therapies, such as probiotics or prebiotics, holds promise for accelerating the restoration of respiratory microbiome eubiosis.

5. Conclusion

In this study, we characterized the disturbance of CAP patients' local microbial and systematic immune response, which persisted at least 4 months post infection compared to healthy controls. These findings deepen our understanding of the dynamic alterations and interactions between the host transcriptome and microbiome during disease course, providing a foundation for future mechanistic research and therapeutic development in CAP.

Ethics statement

This study was approved by the Medical Ethical Committee of China-Japan Friendship Hospital (Beijing, China) and Zibo Municipal Hospital (Zibo, China) (2022-KY-052). All participants were informed about the objective of the study and their right to confidentiality regarding their information. Written informed consent was obtained from each participant.

Acknowledgements

We sincerely thank all the participants, working staff and researchers for their valuable contribution to the study. This work was supported by the National Key R&D Program of China (2022YFA1304303), the Taishan Scholars Program of Shandong Province (tsqn202103196), the National Natural Science Foundation of China (82370017), the Chinese Academy of Medical Sciences (CAMS) Innovation Fund for Medical Sciences (CIFMS 2021-I2M-1-048), and the New Cornerstone Science Foundation.

Conflcit of interest statement

The authors declare that there are no conflicts of interest.

Author contributions

Lizhe Hong: Writing – original draft, Software, Methodology, Formal analysis, Data curation, Conceptualization. **Lijun Suo:** Project administration, Investigation, Conceptualization. **Kang Chang:** Project administration, Investigation, Conceptualization. **Hongyun Cao:** Project administration, Investigation, Conceptualization. **Jiahui Luan:** Project administration, Investigation. **Fuxin Zhang:** Project administration, Investigation. **Xiaofeng Yu:** Project administration, Investigation. **Xiaohui Zou:** Writing – review & editing, Supervision. **Bo Liu:** Writing – review & editing, Supervision. **Bin Cao:** Writing – review & editing, Supervision, Funding acquisition, Conceptualization.

Supplementary data

Supplementary data to this article can be found online at https://doi.org/10.1016/j.bsheal.2025.05.004.

References

[1] R. Lozano, M. Naghavi, K. Foreman, S. Lim, K. Shibuya, V. Aboyans, J. Abraham, T. Adair, R. Aggarwal, S.Y. Ahn, et al., Global and regional mortality from 235 causes of death for 20 age groups in 1990 and 2010: A systematic analysis for the Global Burden of Disease Study 2010, Lancet 380 (2012) 2095–2128, https://doi.org/10.1016/s0140-6736(12)61728-0.

[2] T.P. Meehan, M.J. Fine, H.M. Krumholz, J.D. Scinto, D.H. Galusha, J.T. Mockalis, G.F. Weber, M.K. Petrillo, P.M. Houck, J.M. Fine, Quality of care, process, and outcomes in elderly patients with pneumonia, JAMA 278 (1997) 2080–2084, https://doi.org/10.1001/jama.1997.03550230056037.
[3] C. Troeger, B. Blacker, I.A. Khalil, P.C. Rao, J. Cao, S.R.M. Zimsen, S.B. Albertson, A. Deshpande, T. Farag, Z. Abebe, et al., Estimates of the global, regional, and national morbidity, mortality, and aetiologies of lower respiratory infections in 195 countries, 1990–2016: A systematic analysis for the Global Burden of Disease Study 2016, Lancet Infect. Dis. 18 (2018) 1191–1210, https://doi.org/10.1016/s1473-3099(18)30310-4.
[4] Y. Zhang, Y. Li, N. Sun, H. Tang, J. Ye, Y. Liu, Q. He, Y. Fu, H. Zhu, C. Jiang, J. Xu, NETosis is critical in patients with severe community-acquired pneumonia, Front. Immunol. 13 (2022) 1–13, https://doi.org/10.3389/fimmu.2022.1051140.
[5] B.P. Scicluna, P.M.C. Klein Klouwenberg, L.A. van Vught, M.A. Wiewel, D.S. Ong, A.H. Zwinderman, M. Franitza, M.R. Toliat, P. Nürnberg, A.J. Hoogendijk, et al., A Molecular biomarker to diagnose community-acquired pneumonia on intensive care unit admission, Am. J. Respir. Crit. Care Med. 192 (2015) 826–835, https://doi.org/10.1164/rccm.201502-0355oc.
[6] D. Viasus, A.F. Simonetti, L. Nonell, O. Vidal, Y. Meije, L. Ortega, M. Arnal, M. Bódalo-Torruella, M. Sierra, A. Rombauts, et al., Whole-blood gene expression profiles associated with mortality in community-acquired pneumonia, Biomedicines 11 (2023) 429, https://doi.org/10.3390/biomedicines11020429.
[7] T.J. Marrie, C.Y. Lau, S.L. Wheeler, C.J. Wong, B.G. Feagan, Predictors of symptom resolution in patients with community-acquired pneumonia, Clin. Infect. Dis. 31 (2000) 1362–1367, https://doi.org/10.1086/317495.
[8] R. el Moussaoui, B.C. Opmeer, C.A. de Borgie, P. Nieuwkerk, P.M. Bossuyt, P. Speelman, J.M. Prins, Long-term symptom recovery and health-related quality of life in patients with mild-to-moderate-severe community-acquired pneumonia, Chest 130 (2006) 1165–1172, https://doi.org/10.1378/chest.130.4.1165.
[9] V.F. Corrales-Medina, R.A. deKemp, J.A. Chirinos, W. Zeng, J. Wang, G. Waterer, R.S.B. Beanlands, G. Dwivedi, Persistent lung inflammation after clinical resolution of community-acquired pneumonia as measured by 18FDG-PET/CT imaging, Chest 160 (2021) 446–453, https://doi.org/10.1016/j.chest.2021.02.048.
[10] M.M. Pettigrew, W. Tanner, A.D. Harris, The lung microbiome and pneumonia, J. Infect. Dis.223 (2020) S241–S245, https://doi.org/10.1093/infdis/jiaa702.
[11] H.V. Phan, A. Tsitsiklis, C.P. Maguire, E.K. Haddad, P.M. Becker, S. Kim-Schulze, B. Lee, J. Chen, A. Hoch, H. Pickering, et al., Host-microbe multiomic profiling reveals age-dependent immune dysregulation associated with COVID-19 immunopathology, Sci. Transl. Med. 16 (2024) eadj5154, https://doi.org/10.1126/scitranslmed.adj5154.
[12] L. Ren, Y. Wang, J. Zhong, X. Li, Y. Xiao, J. Li, J. Yang, G. Fan, L. Guo, Z. Shen, et al., Dynamics of the upper respiratory tract microbiota and its association with mortality in COVID-19, Am. J. Respir. Crit. Care Med. 204 (2021) 1379–1390, https://doi.org/10.1164/rccm.202103-0814oc.
[13] J.P. Metlay, G.W. Waterer, A.C. Long, A. Anzueto, J. Brozek, K. Crothers, L.A. Cooley, N.C. Dean, M.J. Fine, S.A. Flanders, et al., Diagnosis and treatment of adults with community-acquired pneumonia an official clinical practice guideline of the american thoracic society and infectious diseases society of America, Am. J. Respir Crit. Care Med. 200 (2019) e45–e67, https://doi.org/10.1164/rccm.201908-1581st.
[14] W.S. Lim, M.M. van der Eerden, R. Laing, W.G. Boersma, N. Karalus, G.I. Town, S. A. Lewis, J.T. Macfarlane, et al., Defining community acquired pneumonia severity on presentation to hospital: an international derivation and validation study, Thorax 58 (2003) 377–382, https://doi.org/10.1136/thorax.58.5.377.
[15] L. Kumar, M.E. Futschik, Mfuzz: A software package for soft clustering of microarray data, Bioinformation 1 (2007) 5–7, https://doi.org/10.6026/9732063000205.
[16] G. Yu, L.G. Wang, Y. Han, Q.Y. He, clusterProfiler: An R package for comparing biological themes among gene clusters, OMICS 16 (2012) 284–287, https://doi.org/10.1089/omi.2011.0118.
[17] A.M. Newman, C.L. Liu, M.R. Green, A.J. Gentles, W. Feng, Y. Xu, C.D. Hoang, M. Diehn, A.A. Alizadeh, Robust enumeration of cell subsets from tissue expression profiles, Nat. Methods 12 (2015) 453–457, https://doi.org/10.1038/nmeth.3337.
[18] W. Mao, E. Zaslavsky, B.M. Hartmann, S.C. Sealfon, M. Chikina, Pathway-level information extractor (PLIER) for gene expression data, Nat. Methods 16 (2019) 607–610, https://doi.org/10.1038/s41592-019-0456-1.
[19] Y. Liu, L. Chen, T. Ma, X. Li, M. Zheng, X. Zhou, L. Chen, X. Qian, J. Xi, H. Lu, et al., EasyAmplicon: An easy-to-use, open-source, reproducible, and community-based pipeline for amplicon data analysis in microbiome research, iMeta 2 (2023) e83, https://doi.org/10.1002/imt2.83.
[20] D.H. Parks, G.W. Tyson, P. Hugenholtz, R.G. Beiko, STAMP: statistical analysis of taxonomic and functional profiles, Bioinformatics 30 (2014) 3123–3124, https://doi.org/10.1093/bioinformatics/btu494.
[21] H.M. Machkovech, A.M. Hahn, J. Garonzik Wang, N.D. Grubaugh, P.J. Halfmann, M.C. Johnson, J.E. Lemieux, D.H. O'Connor, A. Piantadosi, W. Wei, et al., Persistent SARS-CoV-2 infection: significance and implications, Lancet Infect. Dis. 24 (2024) e453–e462, https://doi.org/10.1016/S1473-3099(23)00815-0.
[22] E. Azoulay, L. Russell, A. Van de Louw, L. Russell, A. Van de Louw, V. Metaxa, P. Bauer, P. Povoa, J.G. Montero, I.M. Loeches, S. Mehta, K. Puxty, et al., Diagnosis of severe respiratory infections in immunocompromised patients, Intensive Care Med. 46 (2020) 298–314, https://doi.org/10.1007/s00134-019-05906-5.
[23] R. Karki, T.D. Kanneganti, The 'cytokine storm': molecular mechanisms and therapeutic prospects, Trends Immunol. 42 (2021) 681–705, https://doi.org/10.1016/j.it.2021.06.001.
[24] F. Coperchini, L. Chiovato, G. Ricci, L. Croce, F. Magri, M. Rotondi, The cytokine storm in COVID-19: Further advances in our understanding the role of specific chemokines involved, Cytokine Growth Factor Rev. 58 (2021) 82–91, https://doi.org/10.1016/j.cytogfr. 2020.12.005.
[25] Q. Liu, Y. Zhou, Z. Yang, The cytokine storm of severe influenza and development of immunomodulatory therapy, Cell. Mol. Immunol. 13 (2015) 3–10, https://doi.org/10.1038/cmi.2015.74.
[26] A. Carestia, L.C. Godin, C.N. Jenne, Step up to the platelet: Role of platelets in inflammation and infection, Thromb. Res. 231 (2023) 182–194, https://doi.org/10.1016/j.thromres.2022.10.001.
[27] M.E. Colling, B.E. Tourdot, Y. Kanthi, Inflammation, infection and venous thromboembolism, Circ. Res. 128 (2021) 2017–2036, https://doi.org/10.1161/circresaha.121.318225.
[28] M. Falcone, A. Russo, R. Cangemi, A. Farcomeni, C. Calvieri, F. Barillà, M.G. Scarpellini, G. Bertazzoni, P. Palange, G. Taliani, et al., Lower mortality rate in elderly patients with community-onset pneumonia on treatment with aspirin, J. Am. Heart Assoc. 4 (2015) 1–9, https://doi.org/10.1161/jaha.114.001595.
[29] A.K. Maher, K.L. Burnham, E.M. Jones, M.M.H. Tan, R.C. Saputil, L. Baillon, C. Selck, N. Giang, R. Argüello, C. Pillay, et al., Transcriptional reprogramming from innate immune functions to a pro-thrombotic signature by monocytes in COVID-19, Nat. Commun. 13 (2022) 1–17, https://doi.org/10.1038/s41467-022-35638-y.
[30] P. Severino, E. Silva, G.L. Baggio-Zappia, M.K. Brunialti, L.A. Nucci, O. Rigato Jr., I.D. da Silva, F.R. Machado, R. Salomao, Patterns of gene expression in peripheral blood mononuclear cells and outcomes from patients with sepsis secondary to community-acquired pneumonia, PLoS One 9 (2014) e91886, https://doi.org/10.1371/journal.pone.0091886.
[31] D. Sumbria, E. Berber, M. Mathayan, B.T. Rouse, Virus infections and host metabolism—Can we manage the interactions?, Front Immunol. 11 (2021) 1–14, https://doi.org/10.3389/fimmu.2020.594963.
[32] C. Thibeault, N. Suttorp, B. Opitz, The microbiota in pneumonia: From protection to predisposition, Sci. Transl. Med. 13 (2021) eaba0501, https://doi.org/10.1126/scitranslmed. ba0501.
[33] W.H. Man, W.A.A. de Steenhuijsen Piters, D. Bogaert, The microbiota of the respiratory tract: gatekeeper to respiratory health, Nat. Rev. Microbiol. 15 (2017) 259–270, https://doi.org/10.1038/nrmicro.2017.14.
[34] J.G. Natalini, S. Singh, L.N. Segal, The dynamic lung microbiome in health and disease, Nat. Rev. Microbiol. 21 (2022) 222–235, https://doi.org/10.1038/s41579-022-00821-x.
[35] J. Zhang, Y. Wu, J. Liu, Y. Yang, H. Li, X. Wu, X. Zheng, Y. Liang, C. Tu, M. Chen, et al., Differential oral microbial input determines two microbiota pneumo-types associated with health status, Adv. Sci. 9 (2022) 1–15, https://doi.org/10.1002/advs.202203115.
[36] L.N. Segal, J.C. Clemente, J.C. Tsay, S.B. Koralov, B.C. Keller, B.G. Wu, Y. Li, N. Shen, E. Ghedin, A. Morris, et al., Enrichment of the lung microbiome with oral taxa is associated with lung inflammation of a Th17 phenotype, Nat. Microbiol. 1 (2016) 1–24, https://doi.org/10.1038/nmicrobiol.2016.31.
[37] E.M.M. Quigley, Prebiotics and probiotics in digestive health, Clin. Gastroenterol. Hepatol. 17 (2019) 333–344, https://doi.org/10.1016/j.cgh.2018.09.028.
[38] M.K. Yadav, I. Kumari, B. Singh, K.K. Sharma, S.K. Tiwari, Probiotics, prebiotics and synbiotics: Safe options for next-generation therapeutics, Appl. Microbiol. Biotechnol. 106 (2022) 505–521, https://doi.org/10.1007/s00253-021-11646-8.
[39] A. Tett, E. Pasolli, G. Masetti, D. Ercolini, N. Segata, Prevotella diversity, niches and interactions with the human host, Nat. Rev. Microbiol. 19 (2021) 585–599, https://doi.org/10.1038/s41579-021-00559-y.
[40] I. Brook, Prevotela and Porphyromonas infections in children, J. Med. Microbiol. 42 (1995) 340–347, https://doi.org/10.1099/00222615-42-5-340.
[41] A. Bertelsen, J.S. Elborn, B.C. Schock, Microbial interaction: *Prevotella* spp. reduce *P. aeruginosa* induced inflammation in cystic fibrosis bronchial epithelial cells, J. Cyst. Fibros. 20 (2021) 682–691, https://doi.org/10.1016/j.jcf.2021.04.012.